Sonic Logging in Deviated Boreholes of an Anisotropic Formation: Laboratory Study

Zhenya Zhu, Shihong Chi, and M. Nafi Toksöz

Earth Resources Laboratory
Dept. of Earth, Atmospheric, and Planetary Sciences
Massachusetts Institute of Technology
Cambridge, MA 02139

Abstract

Deepwater field development requires drilling of deviated or horizontal wells. Most formations encountered can be highly anisotropic and P- and S-wave velocities vary with propagation directions. Sonic logs acquired in these wells need to be corrected before they can be applied in formation evaluation and seismic applications. In this study, we make use of a laboratory model made of an approximate transversely isotropic Phenolite to study acoustic logging in deviated wells. We drill holes at various deviations relative to the symmetry axis in the Phenolite block. Then we perform monopole and dipole sonic measurements in these holes and extract the qP, qSV, SH, and Stoneley wave velocities using the slowness-time domain semblance method. The velocities measured using monopole and dipole loggings vary with borehole deviations. We also measure the qP, qSV, and SH wave velocities using body waves at the same angles as the well deviations. We then compute the theoretical qP, qSV, SH, and Stoneley wave velocities based on an equivalent transverse isotropic model of the Phenolite. We find the qP, qSV , and SH wave velocities obtained using the body wave measurement and acoustic logging method agree with the theoretical predictions. The Stoneley wave velocities predicted by the theory also agree reasonably well with the logging measurements.

Introduction

In traditional reservoir development, most wells penetrate the horizontal formations vertically. Sonic well logging measures the P and S wave velocities of the formation in the vertical direction. Deepwater reservoir development requires many deviated wells to be drilled off one platform. Logs acquired in these deviated wells can be significantly different from those in vertical wells since most marine formations show strong anisotropy. Similarly, in fractured reservoirs, formations also show fracture-induced anisotropy. Therefore, it is very important for us to understand what the sonic logging tools measure in these deviated or horizontal wells. Anisotropy correction to well logs is often necessary for constructing correct velocity models for the section (Hornby, 2003). Thus velocities are important both for formation evaluation and for establishing ties to seismic imaging.

The anisotropy of earth material was recognized early in seismic and borehole prospecting methods. Daley and Hron (1977) gave the reflection and transmission coefficients for transversely isotropic (TI) media. Many theoretical studies calculate the

acoustic velocities and waveforms propagating in TI media (White 1982, Thomsen, 1986, Sena and Toksöz, 1993). White et al. (1983) and Issac and Lawton (1999) performed laboratory measurements of the anisotropy in TI media. Zhu et al. (1995) also studied sonic logging in azimuthally anisotropic formations. Hornby (2003) showed significantly improved seismic well ties using anisotropy-corrected sonic logs in deviated wells. Tang and Patterson (2005) demonstrated the apparent anisotropy measured using cross-dipole sonic data in deviated wells could be different from the true formation anisotropy. Chi and Tang (2006) derived the Stoneley wave velocity in deviated wells penetrating anisotropic formations. Therefore, understanding sonic measurements in deviated boreholes drilled in anisotropic formation can provide important insight on applications of sonic logs in offshore fields and fractured reservoir development.

In this study, we use an anisotropic Phenolite as the laboratory material. We first measure the qP, SH, and qSV wave velocities using body waves. We then drill boreholes at different angles with respect to the slowest P-wave principle axis. We record the sonic waveforms measured using a monopole and dipole wireline acoustic logging system in the deviated boreholes. The qP, qSV and SH wave velocities are extracted using the slowness-time semblance method and compared with the velocities measured with body waves.

Industry interpretation of sonic logs acquired in deviated wells often assumes a TI formation model (Hornby et al, 2003, Tang and Patterson, 2005). However, TI formations with differential horizontal stress history or embedded fractures can make the formations show orthorhombic (Shoenberg and Helbig, 1997) or monoclinic anisotropy (Shoenberg and Sayers, 1995). The Phenolite material used in our experiment shows orthorhombic anisotropy. We explore the possibility of using a TI model to interpret our sonic log measurements.

2. Borehole model and measurements

We select a Phenolite CE-578 block with orthorhombic anisotropy for our experiment mainly due to the availability of the material. This Phenolite is made from glass-fiber cloth and epoxy under high pressure. The fibers of the fabric run in two orthogonal directions. One surface of the block is parallel to the fabric layers, and we designate the direction perpendicular to this surface as the Z axis of our coordinate system. The other axes run parallel to the fiber directions and we designate them as the X and Y axes, respectively. These axes are the principle axes of the orthorhombic material. The size of the Phenolite block is 25.4 x 25.4 x 17.8 cm^3. The Phenolite has a density of 1320 kg/m^3.

We use P and S wave transducers to measure the P and S wave velocities along the principle axes of the block. Figure 1 shows velocities along three principal axes. The velocity along the Z axis is 2830 m/s, which is the slowest among the three principal directions for P wave propagation. The P wave velocities along the X and Y axes are 3330 m/s and 3250 m/s, respectively. The S wave velocities along the X, Y and Z axes are 1540 m/s, 1610 m/s, 1440 m/s, respectively. All of the shear wave velocities are very close to the acoustic velocity of water. Both P and S wave velocities are roughly equal in

the X and Y axes direction, respectively, so this Phenolite can be regarded as transversely isotropic with Z as the axis of symmetry. The Thomsen anisotropy (Thomsen, 1986) parameters for P and S waves are about 17.6 % and 9.0%, respectively. Elastic moduli are listed in Table 1.

A cylinder with 24 flat surfaces in 15^{o} azimuthal intervals is cut out of the block along the X axis. The cylinder is 25 cm in length and 17.8 cm in diameter. The distance between the two planes across the center of the cylinder is 17.0 cm (Figure 2).

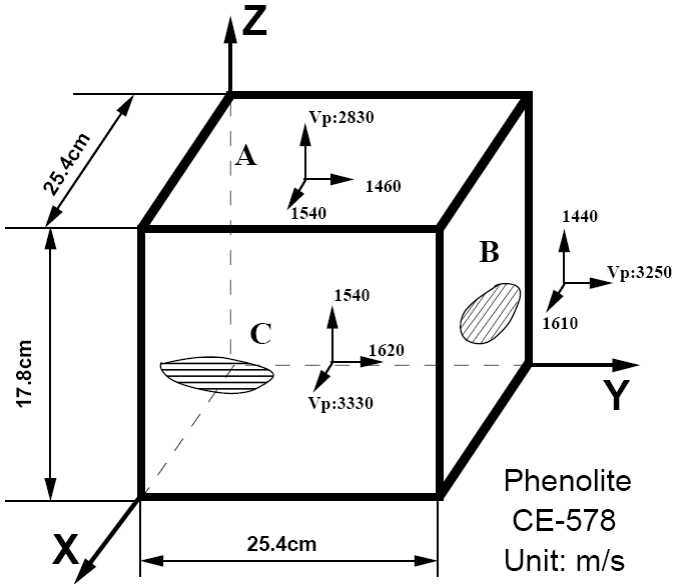

Figure 1. Phenolite CE-578 block and its velocities along its three symmetry axes. The fine layers of the Phenolite block are shown on surfaces B and C. The unit of velocities is in m/s.

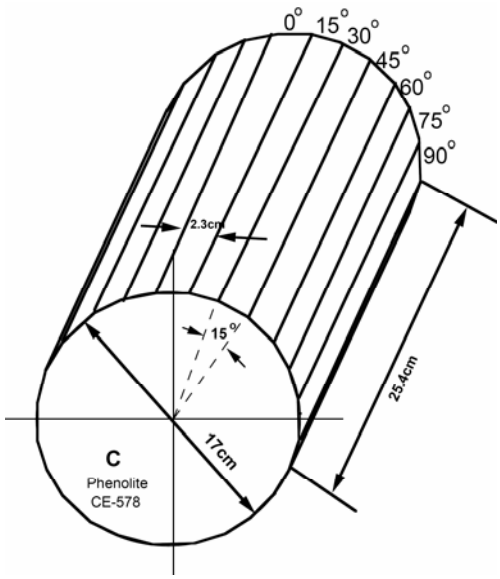

Figure 2. Cylinder model of Phenolite CE-578 along plane C for measuring the P and S wave velocities with body waves. P and S wave velocities at different directions are measured with body wave generated and received with P and S wave transducers.

We measure the velocities between parallel surfaces across the diameter of the cylinder at different angles with respect to the Z axis using two plane P or S wave transducers. When the source transducer is excited by a single sine burst signal, the receiver transducer can record the waveforms propagating through the cylinder along the diagonal direction. Dividing the distance between the two surfaces by the first arrival time of the recorded waveforms recorded by P wave transducers, we obtain the P wave velocity. In the shear wave measurements, we keep the polarization of the shear transducers in the same or opposite directions. We may observe the phase change in the recorded waveforms and determine the arrival times of the shear waves precisely, and then calculate the velocities using the arrival times. Figure 3 shows the P and two shear wave velocities at different angles. The arrows in the coordinate axes indicate the polarizations or the directions of the particle motions. The particle motion of the SH wave is parallel to the cylinder (principal) axis and that of the SV wave is perpendicular to the cylinder axis.

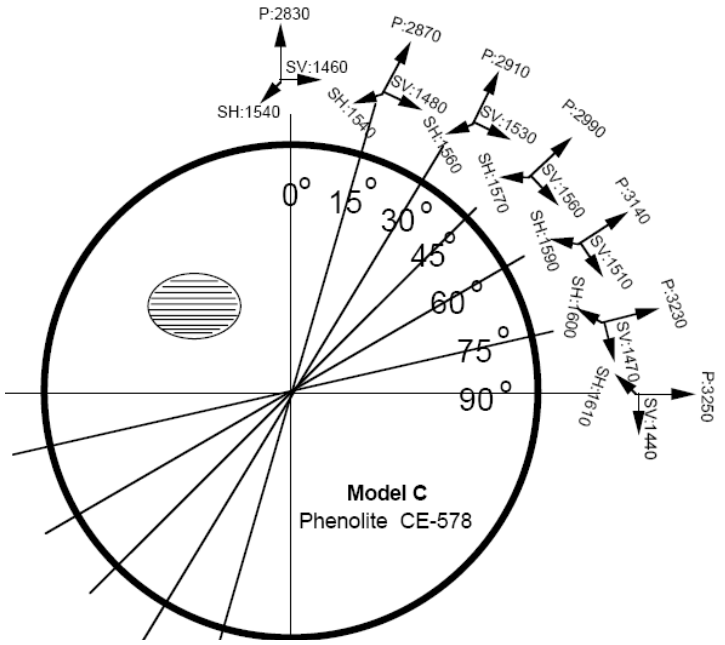

Figure 3. Velocities of the P and S waves measured with the body waves on the Phenolite block at different angles. The unit of the velocities is in m/s.

Figure 4 shows the P wave (a) and two shear wave (b) velocities at different azimuths with respect to the Z axis. P wave velocities increase monotonically from 2830 m/s to 3250 m/s as the azimuth of P wave propagation increase from 0 to 90 degrees. Because of

the anisotropy of the Phelonite block, the shear velocity depends on the polarization and propagation directions. The velocity of the SH wave, whose polarization is parallel to the cylinder axis, is the slowest at 0 degree direction (1540 m/s) and increases up to 1619 m/s at 90 degrees direction. For qSV wave, whose polarization is perpendicular to the cylinder axis, the maximum velocity is measured at 45 degrees (1560 m/s) and the minimum (1450 m/s) is at 0 degree and 90 degrees. The SH velocities are always higher than water velocity (1480 m/s), but the qSV wave velocities are higher or lower than water velocity at different directions.

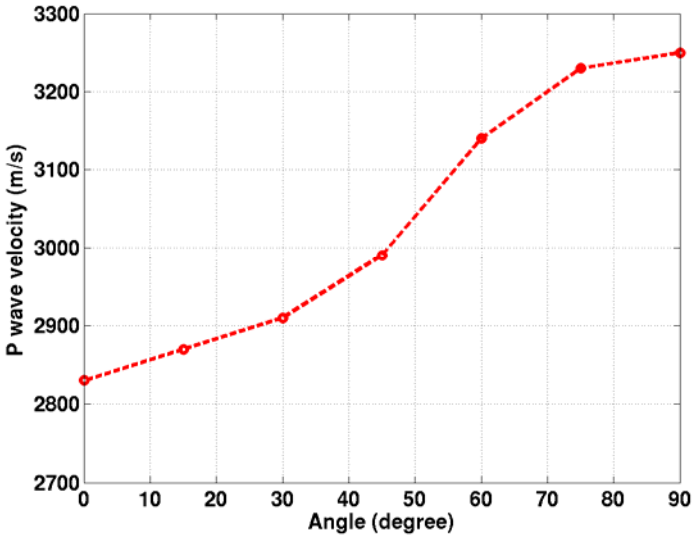

(a)

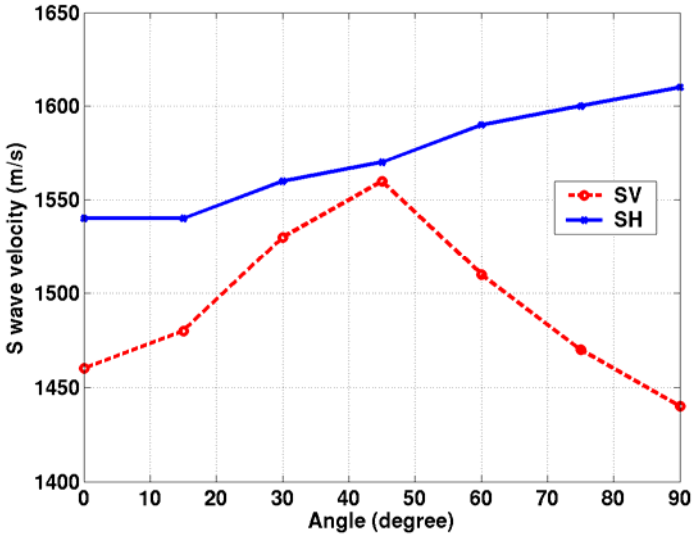

(b)

Figure 4. Velocities of P wave (a) and two S wave (b) measured with body waves on the Phenolite cylinder model at different angle with respect to the Z axis.

Borehole Measurements

Seven boreholes 1.64 cm in diameter are drilled perpendicularly to the cylinder axis at 0, 15, 30, 45, 60, 75 and 90 degrees azimuth (Figure 5). A source monopole or dipole transducer is fixed at a certain position in a borehole and the other monopole or dipole transducer, acting as a receiver, moves along the borehole and records waveforms. The transducer is made of a PZT tube with 0.9 cm in diameter, which is cut into two parts and then is glued together with epoxy. A switch is applied to change the polarizations of the two parts and the transducer can work as a monopole or a dipole transducer to generate or receive the monopole or dipole waves in a borehole. Because a dipole transducer has a polarization direction, a dipole source can be fixed in the direction of the SH or qSV waves and record the flexural waves generated in the two directions. Four sets of the dipole waveforms can be recorded with four combinations of the polarizations of the source and receiver. When we conduct the measurements, the borehole model and the measurement system are immersed in a water tank.

During the borehole measurements, the voltage of the electric signal (a single sine burst) applied to the source is 1.0 V in amplitude and the center frequency is 100 kHz or 200 kHz. Six traces are recorded at 1.0 cm spacing. Each trace has 512 sample points and the sampling rate is 0.3 μs.

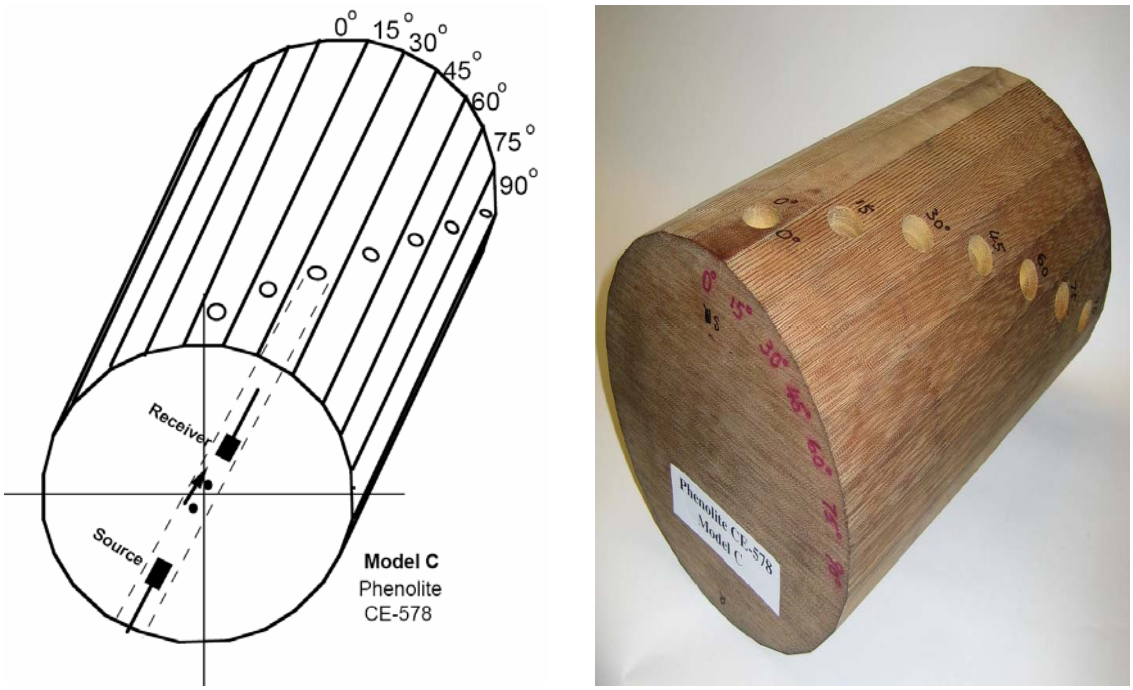

Figure 5. The Phenolite borehole model (a) and its picture (b).

In each borehole of different deviations, we conduct the monopole and dipole logging and record one set of monopole logging data and four sets of the dipole logging data when the dipole source and receiver polarizations are at the fast (F) or slow (S) shear wave directions, respectively. We denote the four sets of dipole data using the combination of the polarizations of the source and receivers as FF, FS, SF, and SS. During the borehole measurements, the source transducer is fixed in the boreholes, and the receiver transducer moves step by step and records the sonic wave in the boreholes at 1.0 cm interval. The smallest receiver-source offset is about 7.0 cm.

In the vertical borehole, monopole array waveforms show P, S, and Stoneley waves (Figure 6). The waves excited by using 100 kHz source have slightly slower group velocity than those of 200 kHz source. However, the waveforms excited by other sources are similar, because the borehole frequency responses are around 100 kHz. The waveforms in the horizontal borehole (Figure 7) show the same modes.

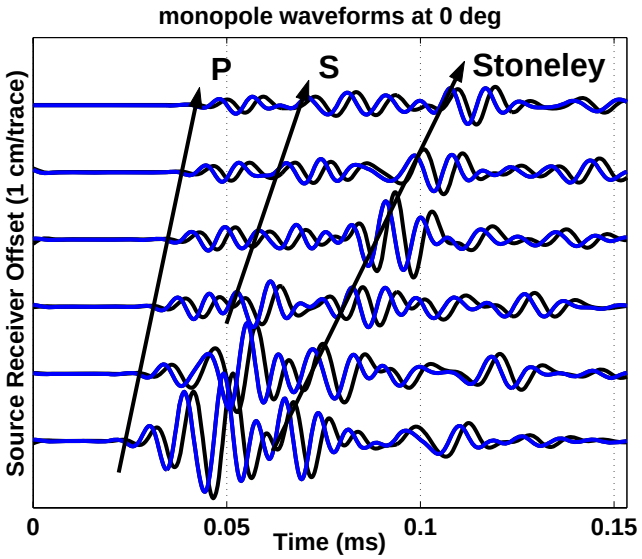

Figure 6. Array waveforms excited by a monopole source in a vertical borehole. The waveforms in black and in blue are excited by using a 100 kHz and 200 kHz source, respectively.

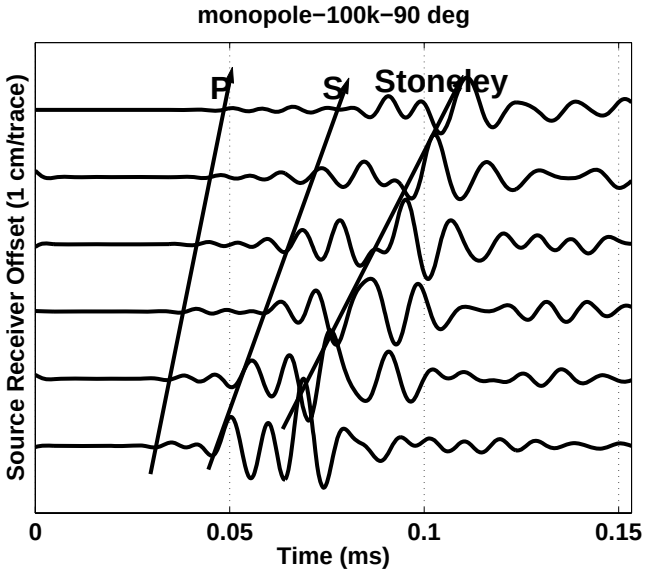

Figure 7. Array waveforms excited by a 100 kHz monopole source in a horizontal borehole.

Dipole waveforms with four different source and receiver orientations (Figure 8) show flexural waves and flexural Stoneley wave. Zhu et al (1995) studied this mode and called it "flexural Stoneley". It has distinctly different particle motion from the flexural wave. It velocity is faster than the Stoneley wave excited in the monopole measurements. Figure 9 shows the waveforms in a horizontal borehole, which have the same flexural and Stoneley modes as those in a vertical borehole.

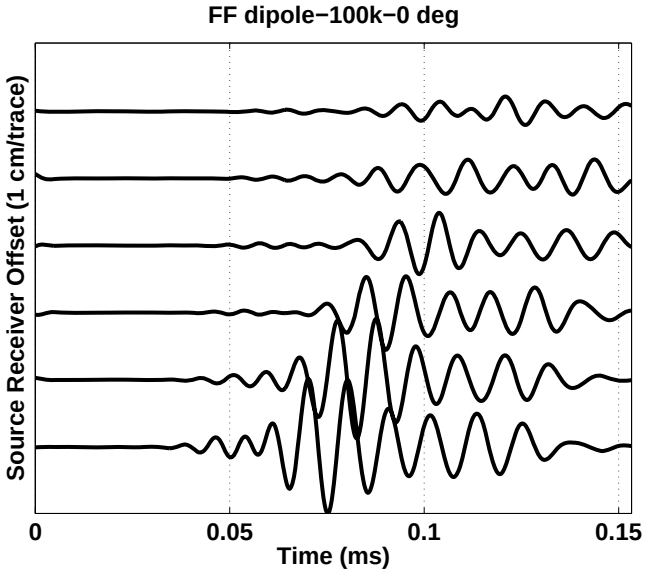

(a)

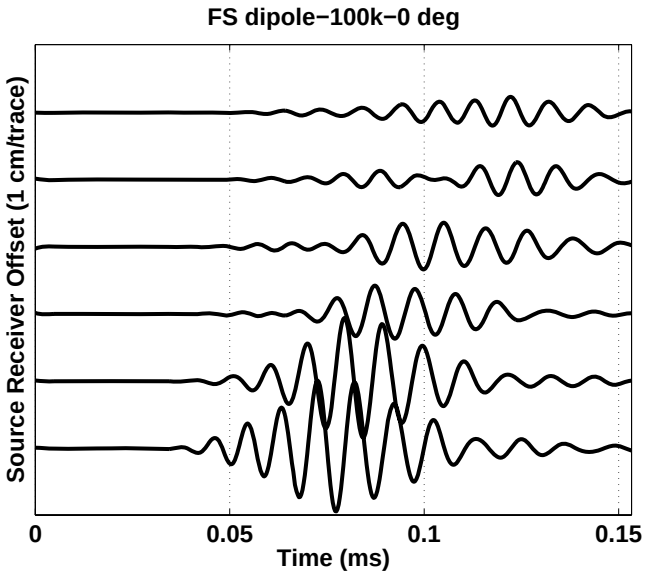
FS dipole−100k−0 deg
Source Receiver Offset (1 cm/trace)
0
0.05
0.1
0.15
Time (ms)

(b)

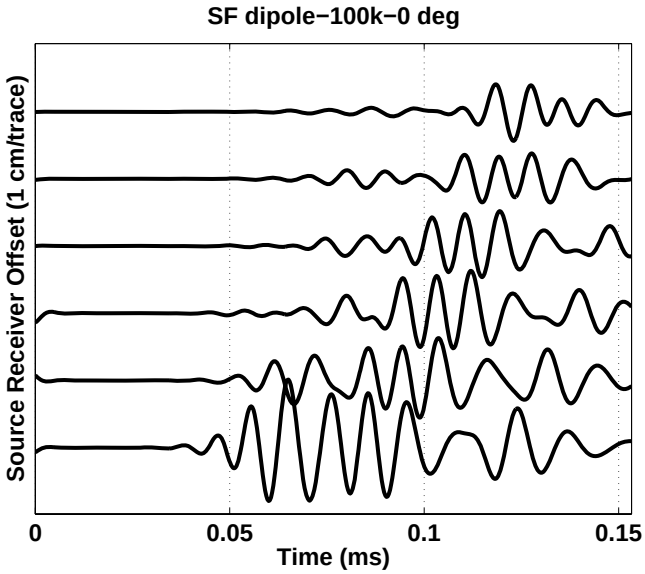
SF dipole−100k−0 deg
Source Receiver Offset (1 cm/trace)
0
0.05
0.1
0.15
Time (ms)

(c)

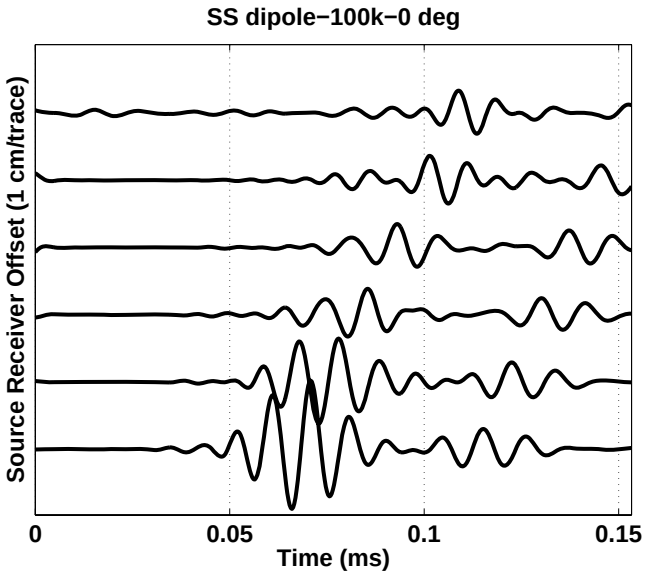

(d)

Figure 9: Dipole waveforms recorded in the vertical borehole using a 100 kHz source.

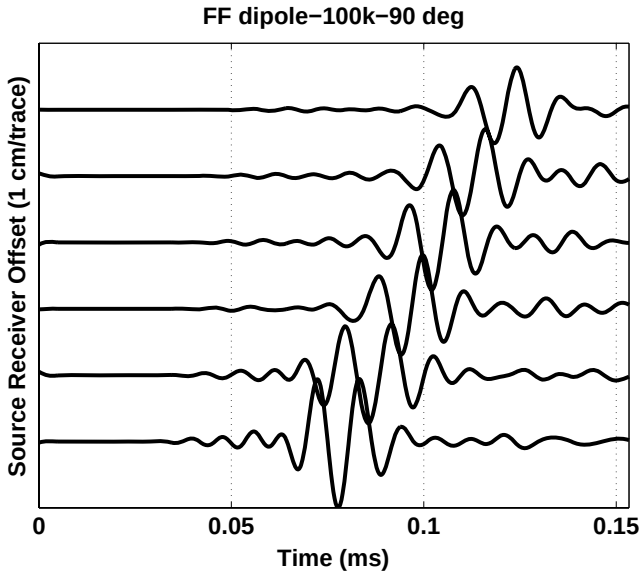

(a)

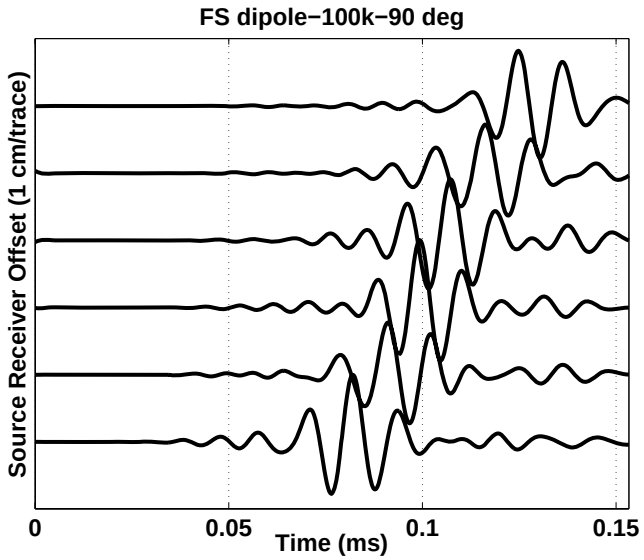
FS dipole−100k−90 deg
Source Receiver Offset (1 cm/trace)
0
0.05
0.1
0.15
Time (ms)

(b)

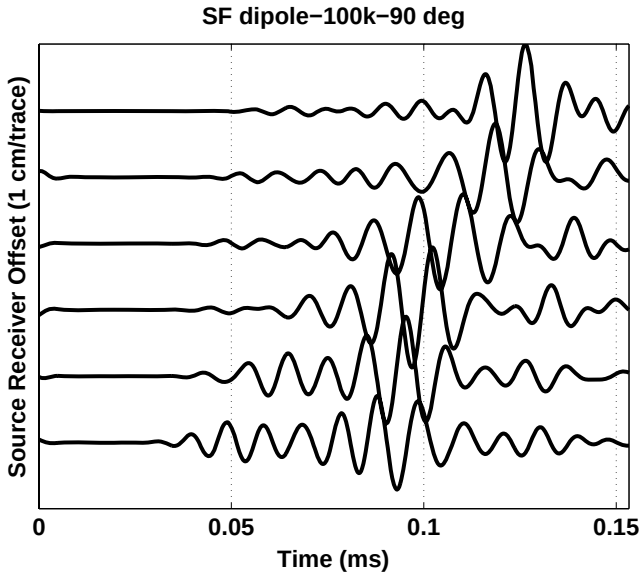
SF dipole−100k−90 deg
Source Receiver Offset (1 cm/trace)
0
0.05
0.1
0.15
Time (ms)

(c)

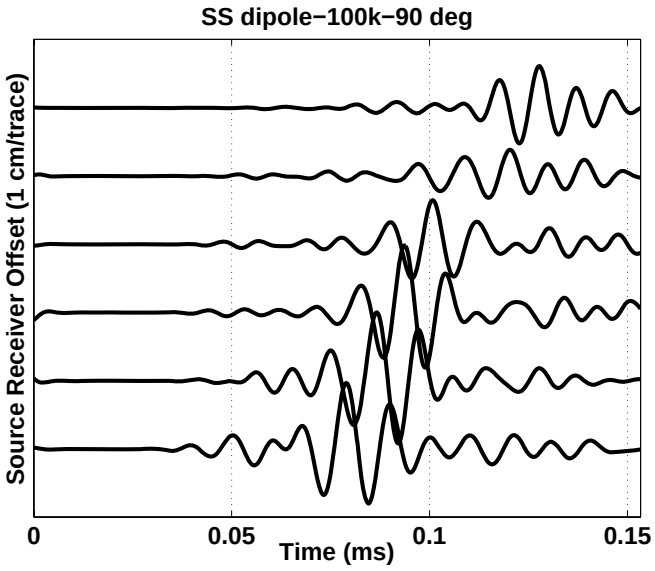

(d)

Figure 10. Dipole waveforms recorded in the horizontal borehole using a 100 kHz source.

Data processing

From the waveforms in the time domain, we can see the different wave modes propagating with the different velocities, and roughly measure the velocities by the slopes of each wave pack. The velocities also can be more accurately determined using the time-domain-semblance method. We perform time domain semblance processing on the received array sonic waveforms. Typical results of the data processing are shown in Figures 11 and 12. Figure 11 shows the monopole waveform recorded in a 75-degree deviated borehole using a 100 kHz source. The semblance plot shows three major peaks for P, S, and Stoneley waves from left to right. The last peak on the upper-right corner is a numerical artifact. Figure 11 shows the dipole waveforms recorded in the 45-degree deviated borehole and the time domain semblance. We see P wave velocity can be determined as well as two shear velocities (Figure 11c). For FF and SS recordings, we expect to receive only fast and slow flexural waves; for FS and SF recordings, we do not expect to excite any flexural waves. However, because the polarizations of the source and receiver are not perfectly linear, detailed semblance processing of the dipole data reveals that both fast and slow shear velocities can be determined, though sometimes the signals are weak due to the limitation of the source and receiver response and borehole geometry.

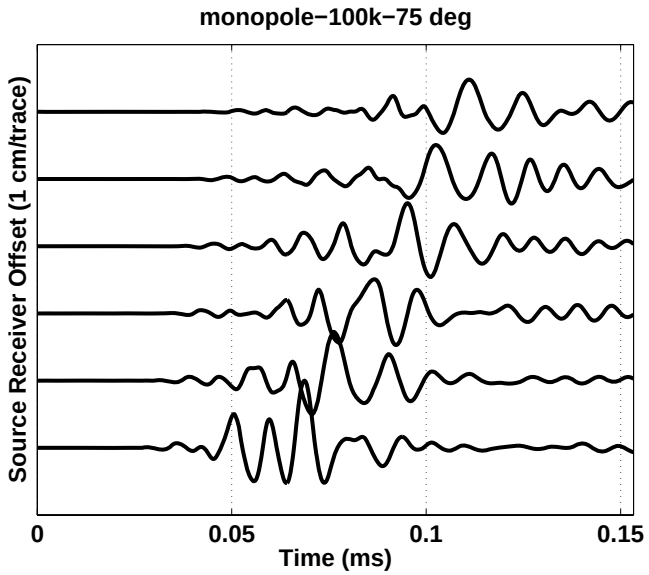

(a)

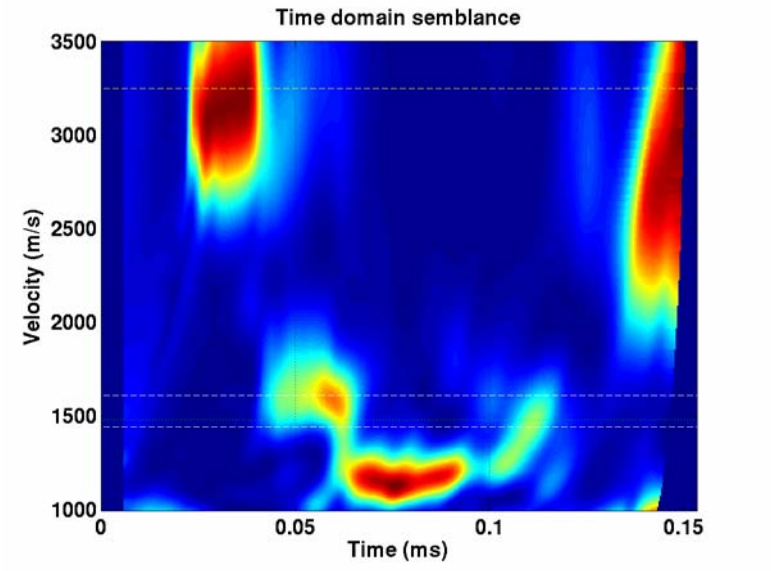

(b)

Figure 11. Acoustic waveforms measured with 100 kHz monopole logging in the borehole at 75-degree deviation (a) and the time domain semblance processing result (b). The dash lines indicate the velocities of the P-wave, fast and slow shear waves, and acoustic velocity in water, measured with the body waves at 75-degree direction.

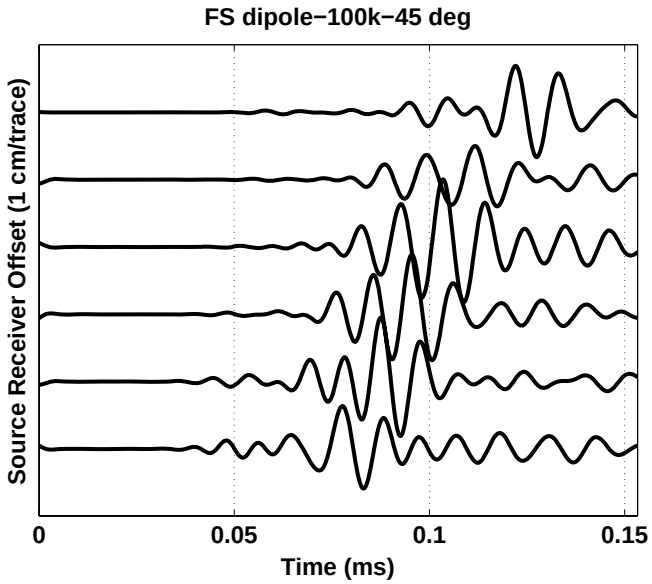
FS dipole−100k−45 deg
Source Receiver Offset (1 cm/trace)
0
0.05
0.1
0.15
Time (ms)

(a)

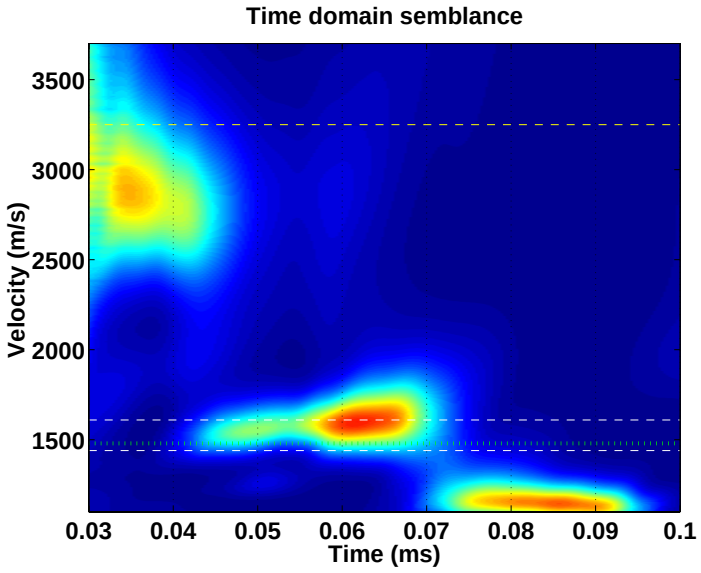
Time domain semblance
Velocity (m/s)
3500
3000
2500
2000
1500
0.03
0.04
0.05
0.06
0.07
0.08
0.09
0.1
Time (ms)

(b)

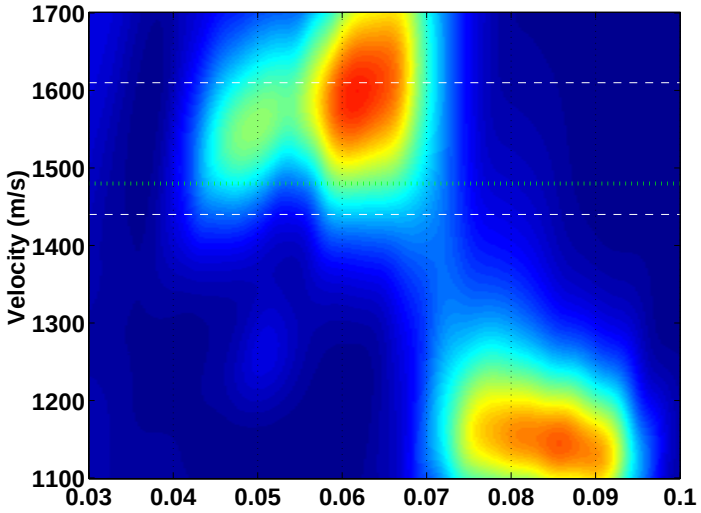

(c)

Figure 12. (a)Acoustic waveforms measured with 100 kHz dipole logging in the borehole at 45-degree deviation, (b) the time domain semblance plot, and (c) the zoom in on the two shear wave peaks. The dash lines indicate the velocities of the qP-wave, fast and slow shear waves, and acoustic velocity in water, measured with the body waves in 45-degree direction.

Therefore, we may determine the qP wave velocity from the monopole or dipole logging data for the material we use; we can determine the fast shear wave velocities from the monopole or dipole logging and the two flexural velocities from the dipole borehole logging. Figure 13a shows the qP wave velocities measured with the body wave and monopole borehole logging. Figure 13b shows the fast (SH wave) velocities measured with monopole borehole logging and slow (SV wave) shear velocities measured with the dipole logging. The log-measured velocities are consistent with those measured directly using the body wave method on the Phenolite block, though in general they are slower. Drilling may have damaged the near-wellbore formation and decreased the logged velocities.

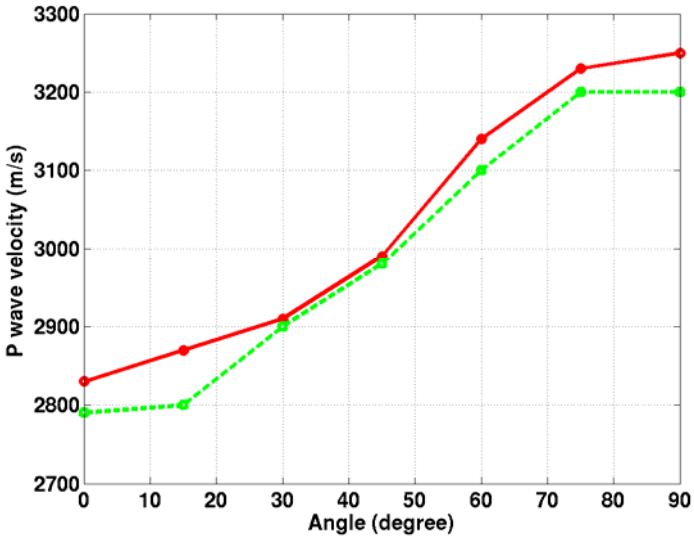

(a)

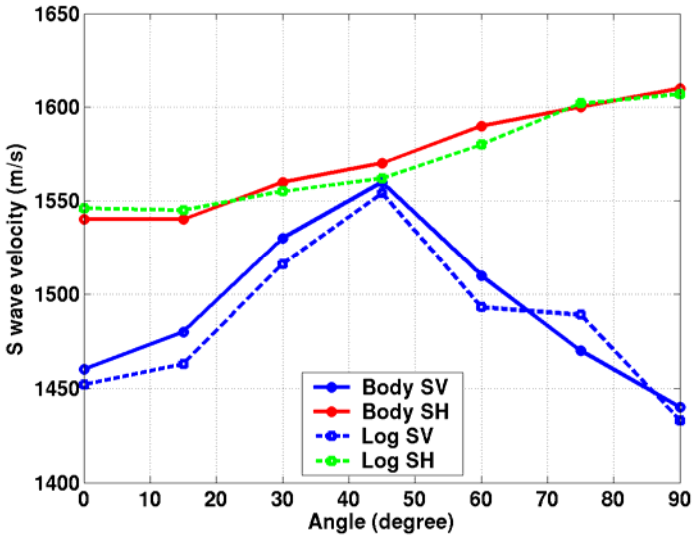

(b)

Figure 13. Velocities of qP wave (a), SH and qSV wave (b) measured in borehole and the velocities measured with the body waves on the model block.

Interpretation of the Measurements using an equivalent TI model

Because of the predominate industry practice using TI models for interpreting sonic logging data, we attempt to find an equivalent TI model for the Phenolite block and see how well the measurements agree with those predicted by the wave propagation theory. We also want to see if we can differentiate an orthorhombic formation from a TI formation.

Based on the dispersion relation of an orthorhombic medium, Schoenberg and Helbig (1997) pointed out that the difference between the orthorhombic equations in a plane symmetry and TI equations in a plane containing the rotational symmetry axis appears only with the inclusion of the cross-plane uncoupled-wave (SH) equation. This is because in general the two shear modes do not have the same velocity even when they propagate in the principal axial directions. And the equations governing the coupled qP and qSV wave in the symmetry plane are exactly the same as those of a TI medium. Since all our boreholes are drilled in the same symmetry plane, we expect a TI model would fit our data well for the qP and qSV waves. The only way we can tell our material is orthorhombic is to use the SH and SV wave data in the vertical borehole.

In TI media, the qP and qSV wave phase velocities are dependent on their propagation direction. Daley and Hron (1977) gave the following formulae:

$$\begin{aligned}\rho V_{qP}^2(\theta) &= \frac{1}{2}\left[c_{33}+c_{44}+(c_{11}-c_{33})\sin^2\theta + D(\theta)\right],\\ \rho V_{qSV}^2(\theta) &= \frac{1}{2}\left[c_{33}+c_{44}+(c_{11}-c_{33})\sin^2\theta - D(\theta)\right],\end{aligned} \tag{1}$$

where ρ is density of the media and phase angle θ is the angle between the wavefront normal and the rotational symmetry axis. $D(\theta)$ is a compact notation for the quadratic combination:

$$\begin{aligned}D(\theta) \equiv \Big\{&(c_{33}-c_{44})^2 + 2\left[2(c_{13}+c_{44})^2 - (c_{33}-c_{44})(c_{11}+c_{33}-2c_{44})\right]\sin^2\theta\\ &+\left[(c_{11}+c_{33}-2c_{44})^2 - 4(c_{13}+c_{44})^2\right]\sin^4\theta\Big\}^{1/2}\end{aligned} \tag{2}$$

and

$$\rho V_{SH}^2 = c_{44}\cos^2\theta + c_{66}\sin^2\theta\,. \tag{3}$$

In our model, the rotational symmetry axis is the Z axis of the coordinate system. We use the P wave velocity along the Y axis as the horizontal P wave velocity. We use the slow S wave velocities, 1460 m/s propagating along the Z axis as the vertical S wave velocity. The vertical P and horizontal S wave velocities are 2830 m/s and 1610 m/s, respectively. From equations (1), (2), and (3), we obtain equations for calculating the vertical and horizontal formation moduli for P and S wave propagation as:

$$c_{44} = \rho V_{SV}^2\,, \tag{4}$$

$$c_{66} = \rho V_{SH}^2\,, \tag{5}$$

$$c_{33} = \rho V_{PV}^2\,, \tag{6}$$

$$c_{11} = \rho V_{PH}^2\,, \tag{7}$$

and

$$c_{12} = c_{11} - 2c_{66}. \tag{8}$$

To solve for c_{13}, we use the qP wave velocity measured at 45 degree deviation and minimize the L-2 norm difference between the theoretically predicted and body wave

measured P wave velocity. Plugging in the velocity measurement and density, we obtain the equivalent elastic moduli for this Phenolite material (Table 1).

c_{11} (GPa)	c_{33} (GPa)	c_{66} (GPa)	c_{44} (GPa)	c_{12} (GPa)	c_{13} (GPa)
13.94	10.57	3.42	2.97	7.10	5.70

Table 1. The elastic stiffness of an equivalent TI model for the Phenolite block

The low frequency Stoneley wave velocity may generally be written as (Norris, 1990):

$$v = \sqrt{\frac{K^*}{\rho_f}}, \tag{9}$$

where ρ_f is the borehole fluid density and the effective Stoneley modulus K^*, which is given by

$$\frac{1}{K^*} = \frac{1}{K_f} + \frac{1}{1-r}\left(\frac{1}{\mu_{fm}} + \frac{r}{\mu_t}\right), \tag{10}$$

where K_f is the bulk modulus of the borehole fluid, r is the volume fraction of the tool relative to the borehole, and μ_{fm} and μ_t are effective formation and logging tool moduli, respectively.

Based on the theory of quasi-static analysis, the effective formation modulus is given by (Chi and Tang, 2003):

$$\mu_{fm} = c_{44}\sin^2\theta + c_{66}\cos^2\theta + \frac{1}{4}\frac{(\varepsilon-\delta)c_{33}\sin^4\theta}{1+2\varepsilon\sin^2\theta/f} \tag{11}$$

where parameters ε, δ, (Thomsen, 1986) and f as follows:

$$\varepsilon = \frac{c_{11}-c_{33}}{2c_{33}}, \tag{12}$$

$$\delta = \frac{(c_{13}+c_{44})^2 - (c_{33}-c_{44})^2}{2c_{33}(c_{33}-c_{44})}, \tag{13}$$

$$f = 1 - \frac{c_{44}}{c_{33}}, \tag{14}$$

Using the estimated TI parameters, we compute the theoretical P, SV, SH, and Stoneley wave velocities with the measurements. Figure 14 shows the comparison of P, SV, and SH wave velocities measured using body wave and logging methods and the theoretical predictions based on an approximated TI model. For the Stoneley wave, we compare the logged and theoretically computed velocities since Stoneley waves only exist in boreholes. Here we do not have a tool body connecting the source and receiver, so we ignore the tool effect on Stoneley wave velocity.

Angle (degree)	0	15	30	45	60	75	90
Body wave P	2830	2870	2910	2990	3140	3230	3250
Log P	2720	2760	2864	2950	3100	3150	3144
Theory P	2830	2843	2892	2990	3113	3212	3250
Body wave SV	1460	1480	1530	1560	1510	1470	1440
Log SV	1452	1463	1516	1554	1493	1489	1433
Theory SV	1460	1494	1554	1574	1538	1484	1460
Body wave SH	1540	1540	1560	1570	1590	1600	1610
Log SH	1546	1545	1555	1562	1580	1602	1607
Theory SH	1460	1471	1499	1537	1574	1600	1610
Log ST	1168	1160	1150	1160	1150	1150	1170
Theory ST	1165	1162	1155	1149	1143	1140	1138

Table 2. Measured velocities of P, SV, SH, and Stoneley waves and their theoretical predictions based on an equivalent TI model. The unit of velocities is m/s.

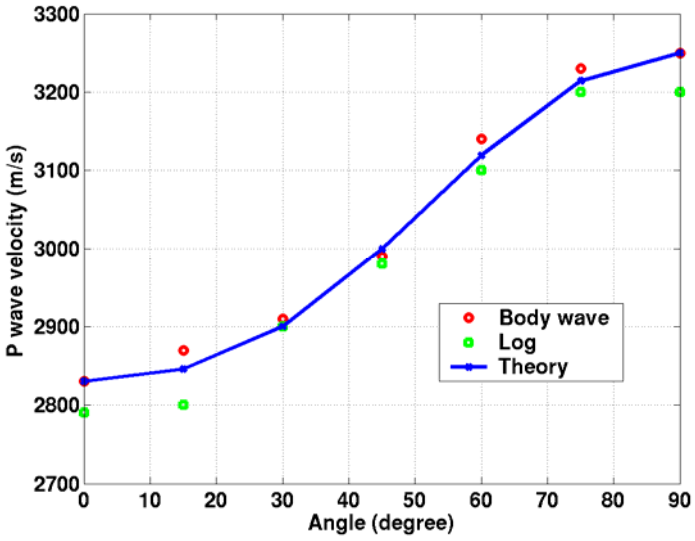

(a)

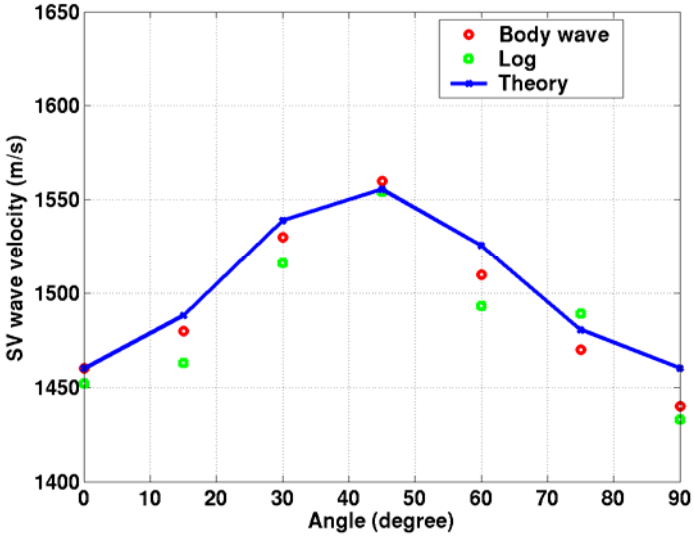
Body wave
Log
Theory
SV wave velocity (m/s)
Angle (degree)
1650
1600
1550
1500
1450
1400
0
10
20
30
40
50
60
70
80
90

(b)

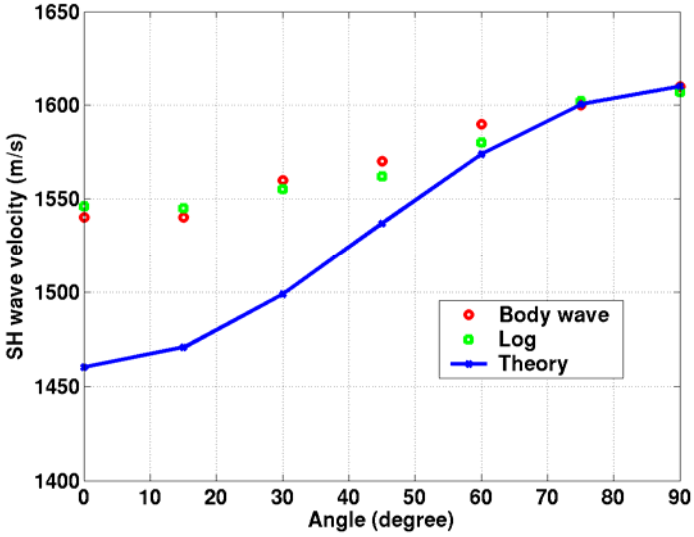
Body wave
Log
Theory
SH wave velocity (m/s)
Angle (degree)
1650
1600
1550
1500
1450
1400
0
10
20
30
40
50
60
70
80
90

(c)

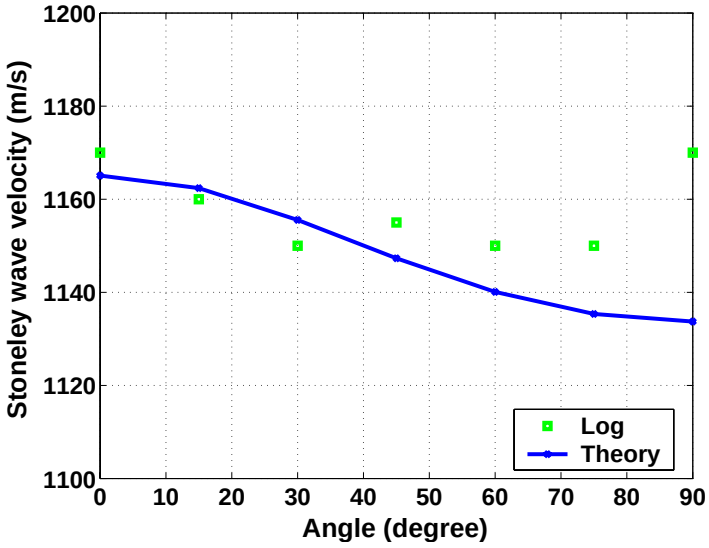

(d)

Figure 14. Comparisons of (a) P-, (b) SV-, and (c) SH-wave velocities measured using body wave and logging methods and the theoretical predictions based on an approximated TI model. (d) shows the comparison for logged and predicted Stoneley wave velocities only.

Figures 14(a) and (b) show that the P and SV wave velocities measured using the body-wave and logging methods and those computed using the theory of wave propagation in a TI medium agree very well. Therefore, the TI model works well for the P and SV waves. The slow shear wave velocity in the XZ symmetry plane controls the SV wave velocity. We can also infer that the elastic stiffness c_{13} is not a critical factor in controlling the P and S wave velocities in deviated wells.

On the other hand, the SH wave velocity at small well deviations below 30 degrees in a TI medium is sensitive to the vertical shear wave velocity, which is slower than the SH velocity 1540 m/s. In our equivalent TI model, we use a vertical shear velocity of 1460 m/s. At higher well deviation, the SH wave velocity becomes more sensitive to the horizontal (fast) shear wave velocity. Therefore, we see the theoretical predictions at high well deviations agree well with the measurements, but at low well deviations, they do not compare well. Figure 15 shows the theoretical SH wave velocities are slower than the SV wave velocities below approximately 55 degree well deviation, and then the SH wave velocities become faster and reach the maximum at 90 degree. Therefore, cross-dipole shear wave anisotropy measurements in deviated wells in a TI formation may jump from negative to positive (Tang and Patterson, 2005). The measurements (Figure 4b) show that the SH wave velocities are consistently higher than those of SV wave at any deviation. Therefore, we do not expect the rapid change in anisotropy with well deviations. In conclusion, when the two shear wave velocities along two principal axes differ considerably, using acoustic logging measurement, we can differentiate a TI formation from an orthorhombic one. When data in vertical boreholes are not available, changes in cross-dipole anisotropy may give us useful insight.

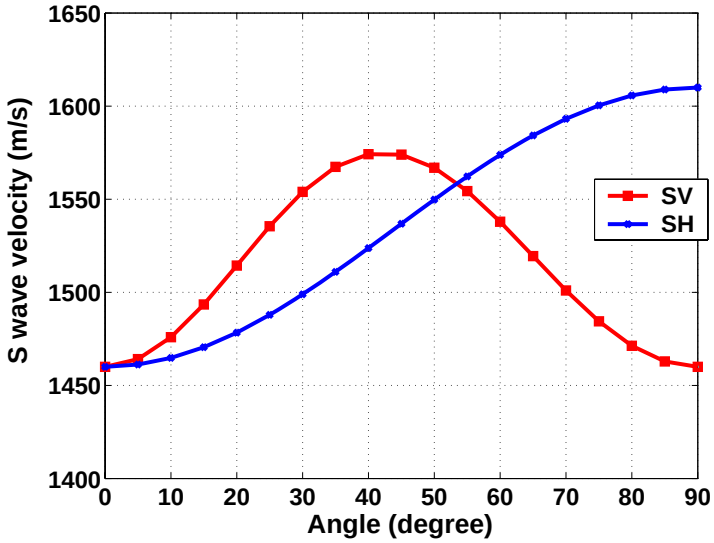

Figure 15. Theoretical SV and SH wave velocity variations with borehole deviations.

In theory, at small well deviations below 30 degrees, Stoneley wave velocities are sensitive to that of the horizontal shear wave; at higher well deviation, Stoneley wave velocity becomes more sensitive to the vertical shear wave velocity. Stoneley wave velocity decreases with borehole deviation. However, the highest Stoneley velocity in the vertical borehole is 2.9% higher than that in the horizontal borehole. The logging measurements seem to agree with the theory in the general trend, but the changes in Stoneley wave velocity are relatively small and they are within the measurement errors. The maximum difference between the theoretically computed and the log derived Stoneley wave velocities is about 2% in the horizontal borehole. It seems the theory on Stoneley wave velocity agrees with the logging measurements in general, but further validation using materials that have strong shear wave anisotropy is necessary.

5. Conclusions

We used an anisotropic (approximately TI) Phenolite block to drill seven boreholes at different angles inclination relative to the symmetry axis, and carried out monopole and dipole acoustic logging measurements. We determined the qP and SH wave velocities with monopole logging and qSV wave velocity with dipole logging. The velocities of qP, SH, and qSV waves measured on the cylinder block and in the boreholes agree well.

For the Phenolite, we calculated the phase velocities of qP, SH and qSV waves in the TI medium theoretically. The velocities of qP and qSV waves measured on the cylinder block and in the boreholes agree with the theoretical results. The measured SH wave velocities at small phase angles are sensitive to the intermediate fast shear wave velocity and therefore are much faster than the slow shear wave as predicted by the theory due to the assumption of TI material. The Stoneley velocities measured in boreholes agree with the trend predicted by the theory.

Our results are helpful for the interpretation of the log-derived velocities measured in deviated wells penetrating an anisotropic formation.

6. Acknowledgements

We thank Rama Rao and Daniel Burns for their valuable suggestions and useful discussions. This work is supported by the Earth Resources Laboratory Borehole and Acoustic Logging Consortium and Founding Member Consortium.

7. References

1. Brian, E. H., Howie, J. M., and Ince, D. W., 2003, Anisotropy correction for deviated-well sonic logs: Application to seismic well tie. Geophysics, 464-471.
2. Chi, S., and Tang, X. M., 2003, Accurate approximations to qSV and qP wave speeds in TIV media and Stoneley wave speed in general anisotropic media: 44th Annual Logging Symposium, Society of Professional Well Log Analysis, Paper OO.
3. Chi, S., and Tang, X. M., 2006, Stoneley wave speed in general anisotropic formations, accepted for publication by Geophysics.
4. Daley, P. F., and Hron, F., 1977, Reflection and transmission coefficients for transversely isotropic media, Bull. Seism. Soc. Am., 67, 661-675.
5. Hornby, B. E., Howie, J. M.. Ince, D. W., Anisotropy correction for deviated-well sonic logs: Application to seismic well tie, Geophysics, 68, 464-471.
6. Isaac, J. H., and Lawton, D. C., 1999, Image mispositioning due to dipping TI media: A physical model seismic modeling study: Geophysics, 64, 1230-1238.
7. Schoenberg, M., and Helbig, K., 1997, Orthorhombic media: modeling elastic wave behavior in a vertically fractured earth, Geophysics, 62, 1954-1974.
8. Schoenberg, M. and C. M. Sayers, 1995, Seismic anisotropy of fractured rock, Geophysics, 60, 204-211.
9. Sena, A. G., and Toksöz, M. N., 1993, Kirchhoff migration and velocity analysis for converted and nonconverted waves in anisotropic media: Geophysics, 58, 265-276.
10. Tang, X. M., and Patterson, D., 2005, Characterizing seismic anisotropy using cross-dipole measurement in deviated wells, SEG Annual Meeting, Houston.
11. Thomsen, L., 1986, Weak elastic anisotropy: Geophysics, 51, 1954-1966.
12. White, J. E., 1982, Computed waveforms in transversely isotropic media: Geophysics, 47, 771-783.
13. White, J. E., Martineau-Nicoletis, L., and Monash, C., 1983, Measured anisotropy in Pierre Shale, Geophys. Prosp., 31, 709-725.
14. Zhu, Z., Cheng, C. H., and Toksoz, M., N., 1995, Polarization of flexural waves in an anisotropic borehole model. 65th SEG Annual Meeting, Expanded Abstracts, BG3.8, 89-92.